Elucidation of novel 13-series resolvins that increase with atorvastatin and clear infections

Jesmond Dalli[1], Nan Chiang[1] and Charles N. Serhan[1]

[1]Center for Experimental Therapeutics and Reperfusion Injury, Department of Anesthesiology, Preoperative and Pain Medicine,
Harvard Institutes of Medicine, Brigham and Women's Hospital
and Harvard Medical School, Boston, Massachusetts.

Correspondence should be addressed to: Prof. Charles N Serhan,
E-mail: cnserhan@zeus.bwh.harvard.edu; Tel: 617-525-5001; Fax: 617-525-5017

Supplementary Figures

Supplementary Figure 1: Neutrophil-endothelial cell products do not display direct antibacterial actions. (**a**) Fractions were extracted from human (h) neutrophil (PMN)-endothelial cell (EC) co-incubations (see methods). These products or ampicillin (1mM) were placed on GF-C filters then on LB agar plates containing *E. coli* ($1x10^7$ CFU). The zone of clearance was assessed after overnight incubation at 37°C. Results are representative of three independent experiments. (**b**) Proposed structures and biosynthetic scheme for 13-series resolvins (RvT)

Supplementary Figure 2: Identification of novel n-3 docosapentaenoic acid derived 13-series resolvins in neutrophil endothelial co-incubations. (**a-d**) Fractions were extracted from human neutrophil (hPMN)-endothelial cell (hEC) co-incubations (see methods). Mediators were profiled using lipid mediator (LM) metabololipidomics. MS-MS fragmentation spectra employed for identification of (**a**) 13-series resolvin (RvT) 1, (**b**) RvT2, (**c**) RvT3 and (**d**) RvT4. Results are representative of n=4 independent cell incubations. (**e**) hEC were incubated with IL-1β and TNF-α (10ng/ml each, 16h, 37°C), then with vehicle (PBS plus 0.01% EtOH), 1μM EPA, n-3 DPA or DHA (15min, 37°C) and human neutrophils (hPNM; $1x10^7$ cells/ml, 60min, 37°C). Fractions were extracted using solid phase extraction columns, identified and quantified using LC-MS-MS (see methods for details). Results are mean±s.e.m. n=3 cell preparations from two independent experiments. *p<0.05, **p<0.01 *vs* hPMN-EC incubations. (**f**) hEC), hPMN and hPMN-EC were incubated with n-3 DPA (see methods for details) and RvT identified and quantified using LC-MS-MS based LM metabololipidomics. RvT1, RvT2, RvT3 and RvT4 levels identified in neutrophil-endothelial cell co-cultures. Results are mean±s.e.m.

n=4 cell preparations per group from four independent experiments. *p<0.05 *vs.* amounts in hEC.

Supplementary Figure 3: Human COX-2 converts n-3DPA to 13R-HDPA in endothelial cells. (**a**) Human endothelial cells (hEC) were incubated with IL-1β and TNF-α (10ng/ml each, 16h, 37°C) followed by vehicle (PBS containing 0.01% EtOH) or n-3 DPA (1μM, 60 min, 37°C). Fractions were extracted (see methods) and 13-HDPA was profiled using LM metabololipidomics. Results are mean±s.e.m. n=4 cell preparations from four independent experiments. *p<0.05 *vs.* hEC plus vehicle cells. (**b**) MRM chromatograms for standard 13R-HDPA and 13S-HDPA from chiral LC-MS-MS. (**c,d**) hEC were incubated as in (**a**) and 13-HDPA was assessed by chiral LM metabololipidomics. (**c**) MRM chromatogram for ion pair m/z 345>195 (**d**) MS-MS spectrum employed in the identification of 13R-HDPA. Results for (c,d) are representative of n=4 cell preparations from four independent experiments. (**e**) hEC were incubated with IL-1β and TNF-α (10ng/ml each, 16h, 37°C) followed by vehicle (PBS containing 0.01% DMSO) or celecoxib (25μM, 25min, 37°C); n-3 DPA (1μM, 60min, 37°C) was then added, products extracted and 13-HDPA levels determined by LM metabololipidomics. (**f**) Endothelial cells were transfected with control scrambled (CS) or human COX-2 shRNA; cells were then incubated with IL-1β and TNF-α (10ng/ml each, 16h, 37°C) and n-3 DPA (1μM, 60min, 37°C). 13-HDPA levels were determined by LM metabololipidomics. Results for (e,f) are mean±s.e.m. n=4 cell preparations from four independent experiments. For (e) *p<0.05 *vs.* IL-1β plus TNF-α incubations alone. For (f) *p<0.05 vs. CS-shRNA plus IL-1β and TNF-α incubations. (**g-h**) Human recombinant (hr) COX-2 was incubated with n-3 DPA or AA (0.1M Tris-HCl, pH8.0, 20μM porcine hematin, 0.67mM phenol, Room Temperature, 60min) at the indicated concentrations

and product formation was assessed (see methods) using (**g**) chiral LM metabololipidomics for hrCOX-2 products from n-3 DPA. (**h**) Michaelis Menten kinetics. Results for (g) are representative of n=6 incubations; (h) are mean±s.e.m. n=6 incubations from three independent experiments.

Supplementary Figure 4: Physical characteristics of RvT1, RvT2, RvT3 and RvT4. 13R-HDPA was incubated with potato 5-LOX (0.1M phosphate buffer, pH 6.3, 0.03% Tween 20, 30min); products were isolated using RP-UV-HPLC (see methods for details). (**a-d**) In phase, online UV-chromophores recorded for (**a**) RvT1, (**b**) RvT2, (**c**) RvT3, (**d**) RvT4. (**e-h**) Isolated products were incubated with diazomethane in ether (30min, Room Temperature) and assessed by LM metabololipidomics. MS-MS fragmentation spectra for the sodium adducts of (**e**) RvT1-methyl ester, (**f**) RvT2-methyl ester, (**g**) RvT3-methyl ester and (**h**) RvT4-methyl ester. Results are representative of three independent experiments.

Supplementary Figure 5: Molecular oxygen incorporation demonstrates a role for neutrophil lipoxygenases in the biosynthesis of the novel RvT. Human peripheral blood neutrophils ($5x10^7$/ml) were incubated with 13-HPDA (75ng/ml; $PBS^{+/+}$; pH7.45) in an atmosphere enriched in $^{18}O_2$. *E. coli* were then added ($2.5x10^9$/ml), incubations quenched after 30min (37^oC) using 2 volumes of ice-cold methanol and products reduced using sodium borohydride (1µg/ml, 15min, 4^oC). Products were extracted, and identified using LC-MS-MS. (**a-d**) Representative structures and MS-MS spectra employed in the identification of (**a**) RvT1, (**b**) RvT2, (**c**) RvT3 and (**d**) RvT4. Results are representative of 4 neutrophil preparations from four independent experiments.

Supplementary Figure 6: Trapping products indicate the formation of an epoxide intermediate in RvT2 and RvT3 biosynthesis. Human neutrophils ($5x10^7$ cells/ml) were incubated with 13R-HDPA (1μM, 37°C, PBS pH 7.45) and *E. coli* ($1x10^9$ CFU/ml, 2min, 37°C). Incubations were stopped with 2 volumes of acidified methanol (apparent pH 3), the products extracted and profiled using LM metabololipidomics. (**a**) MRM chromatogram for the methoxy-trapping products of RvT2 (left panel) and MS-MS spectra (right panel). (**b**) MRM chromatogram for the methoxy-trapping products of RvT3 (left panel) and MS-MS spectra (right panel). Results are representative of three independent experiments.

Supplementary Figure 7: Inhibition of nitric oxide synthase reverts atorvastatin mediated increases in RvT. (**a**) Human (h) endothelial cells (EC) were incubated with IL-1β and TNF-α (10ng/ml each, 16h, 37°C), vehicle (PBS containing 0.01% DMSO), L-NAME (25μM) or 1400W (10μM, 25min, 37°C). Atorvastatin (atorv; 30μM, 30min), n-3 DPA (1μM, 15min, 37°C) and PMN ($1x10^7$ cells/ml, 60min, 37°C) were then added, fractions were isolated and profiled using LM metabololipidomics. Results are mean±s.e.m. n=4 independent incubations from four independent experiments. *$p<0.05$, *vs.* hPMN-EC incubations. #$p<0.05$ *vs* hPMN-EC plus atorvastatin incubations. (**b**) Human recombinant COX-2 was incubated without (COX-2) or with S-nitrosoglutathione (COX-2+GSNO) prepared as detailed in the methods section for 30min (Room Temperature). S-nitrosylation was then assessed using Western blotting (see methods for details). Results are representative of n= 6 incubations and three independent experiments.

Supplementary Figure 8: RvT regulate inflammasome components in human macrophages and mice during *E.coli* infections. Macrophages (MΦ; $1.5x10^5$

cells/well) were incubated with the indicated concentrations of RvT1, RvT2 plus RvT3 (1:1 ratio), RvT4 or vehicle (PBS containing 0.01% EtOH; 15min, 37^{o}C, pH 7.45), *E.coli* were added (1.5x10^{7} CFU/well, 16h, 37^{o}C, pH 7.45) and (**a**) caspase 1 levels assessed by flow cytometry; (**b**) IL-1β levels and (**c**) LDH activity were measured in the supernatants. Results are expressed as mean±s.e.m. n=4 donors from three independent experiments. *p<0.05, **p<0.01, ***<0.001 *vs.* macrophages plus *E.coli;* ##p<0.01 *vs.* macrophages alone. Mice were given vehicle (saline containing 0.1% EtOH) or a combination of RvT1, RvT2, RvT3 and RvT4 (at a ratio of 2:1:1:8), which were each isolated and quantified by RP-UV-HPLC (see methods for details) *via i.p*. injection 2h post *E.coli* (1x10^{7} CFU/mouse) inoculation; 12h later (**c**) exudate monocyte/macrophage caspase 1 expression, (**d**) exudate IL-1β levels, (**e**) exudate lactate dehydrogenase activity and (**f**) peripheral blood leukocyte-platelet aggregates were determined. Results are mean± s.e.m. n=5 mice per group from two independent experiments. *p<0.05, **p<0.01 *vs. E.coli* mice.

Supplementary Figure 9: RvT regulate exudate eicosanoids and do not display antibacterial actions at bioactive concentrations. (**a**) RvT were isolated and quantified using RP-UV-HPLC. RvT1, RvT2 plus RvT3, RvT4 (10μM) or ampicillin (10mM) were placed on LB agar plates containing *E. coli* (1x10^{7} CFU). The zone of clearance was assessed after overnight incubation at 37^{o}C. Results are representative of three independent experiments. (**b**) Mice were given a combination of RvT1, RvT2, RvT3 and RvT4 (RvT; 125ng each/mouse; *i.p.*); each was isolated and quantified using RP-UV-HPLC (see methods for details), then combined in a mixture or vehicle (saline containing 0.1% EtOH) 5 min prior to *E.coli* (1x10^{7} CFU/mouse) inoculation; 12h later peritoneal exudates were collected and LM profiled using LM metabololipidomics.

Results are mean±s.e.m. n=4 mice per group from two independent experiments. *p<0.05; **p<0.01 *vs. E.coli* mice.

Supplementary Figure 10: Atorvastatin and RvT reduce local and systemic inflammation in murine infections. Mice were administered a combination of RvT1, RvT2, RvT3 and RvT4 (RvT ~12.5ng/mouse each); each was isolated and quantified using RP-UV-HPLC (see methods for details) and/or atorvastatin (atorv; 0.5µg/mouse *i.p.)* or vehicle (saline containing 0.1% EtOH) 5 min prior to *E.coli* inoculation ($1x10^7$ CFU/mouse*; i.p*). Twelve hours later (**a**) peritoneal exudate neutrophil counts, (**b**) exudate bacterial loads, (**c**) peripheral blood bacterial loads, (**d**) exudate IL-1β levels, (**e**) exudate lactate dehydrogenase activity, (**f**) bacterial phagocytosis by peritoneal leukocytes, and (**g**) macrophage efferocytosis in peritoneal exudates were measured. Results are mean±s.e.m. n=4 mice per group, from two independent experiments. *p<0.05 , **p<0.01 *vs. E.coli* mice. (**h-k**) Mice were inoculated with *E.coli* ($1x10^7$ CFU/mouse*; i.p.*); 2h later administered RvT1, RvT2, RvT3 and RvT4; each was isolated and quantified using RP-UV-HPLC (see methods for details), then combined in a mixture at a ratio of 2:1:1:8 (RvT; total 50ng/mouse) and/or atorvastatin (atorv; 0.5µg/mouse *i.p.)* or vehicle (saline containing 0.1% EtOH). (**h**) Twelve hours later, peritoneal exudate neutrophil counts (left panel) and exudate bacterial loads were measured (right panel). (**i-k**) Six hours after *E.coli* administration (**i,k**), peripheral blood eicosanoid levels were measured using LC-MS-MS or ELISA; (**j**) Lung mRNA levels of endothelin (ET)-1 and plasminogen activator inhibitor (PAI) were measured using qRT-PCR. *p<0.05, **p<0.01, ***p<0.001 *vs. E.coli* mice; #p<0.05 *vs. E.coli* plus RvT mice; § p<0.05 *vs. E.coli* plus atorvastatin mice. Results for a-e are mean±s.e.m. n=5 mice per group from two independent experiments.

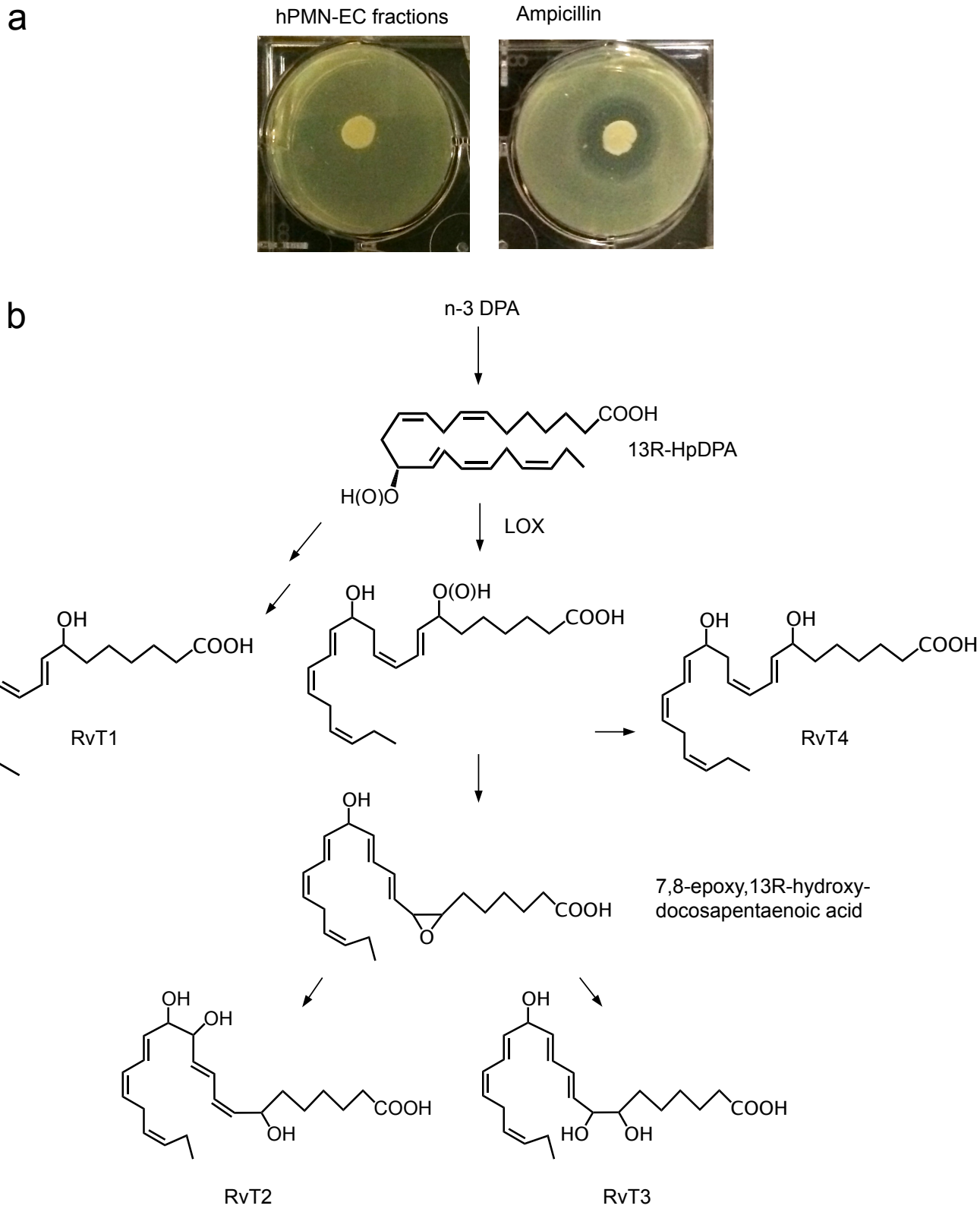
a
hPMN-EC fractions
Ampicillin
b
n-3 DPA
COOH
13R-HpDPA
H(O)O
LOX
OH
OH
COOH
RvT1
OH
O(O)H
COOH
OH
OH
COOH
RvT4
OH
COOH
O
7,8-epoxy,13R-hydroxy-
docosapentaenoic acid
OH
OH
COOH
OH
RvT2
OH
HO
OH
COOH
RvT3

Supplementary Figure 2

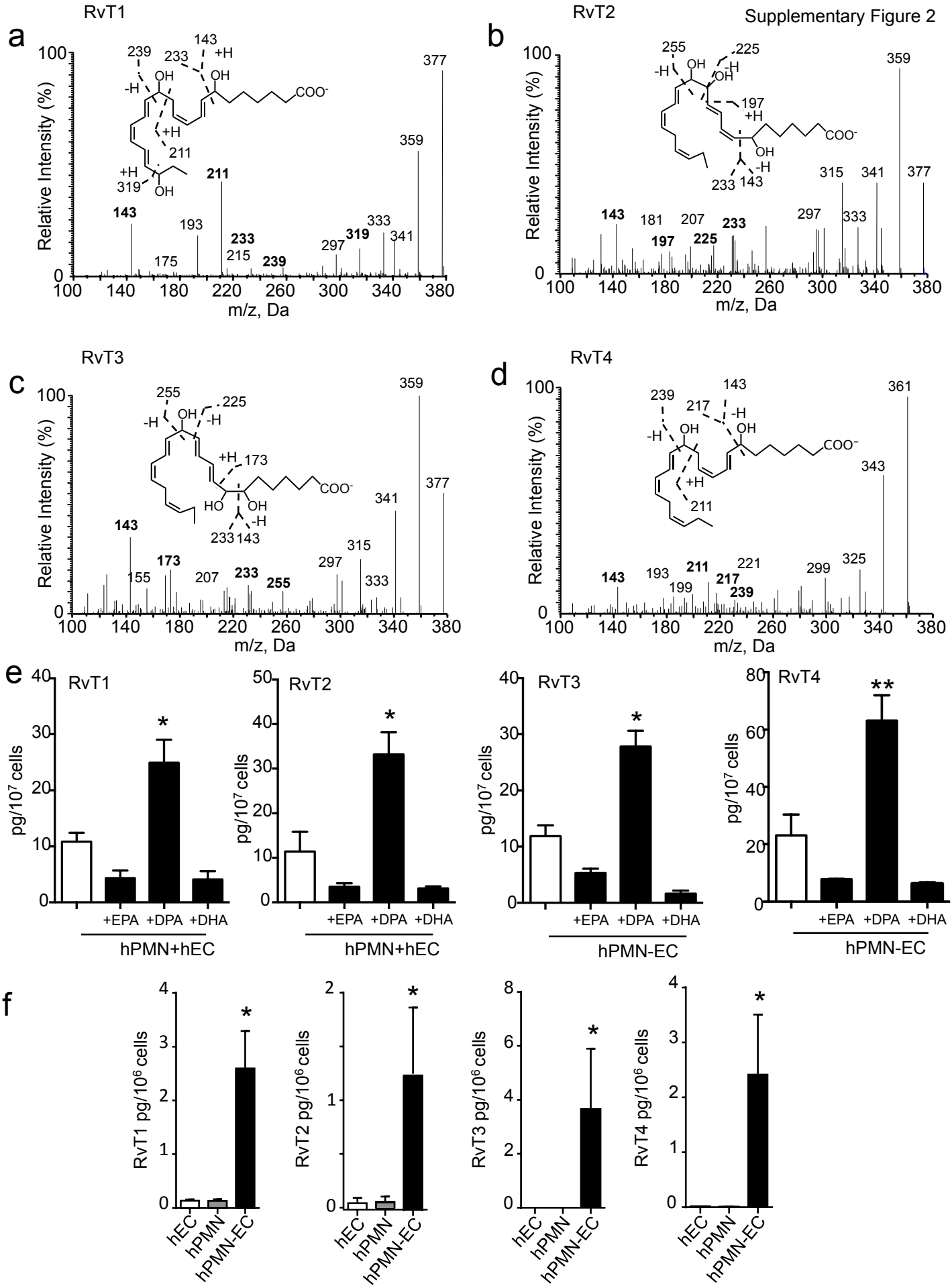

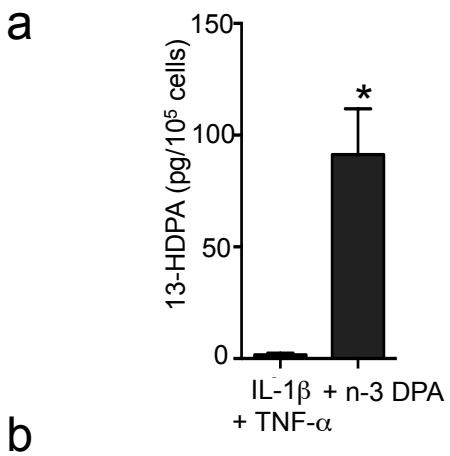
a
13-HDPA (pg/10^5 cells)
150
100
50
0
*
IL-1β + n-3 DPA
+ TNF-α

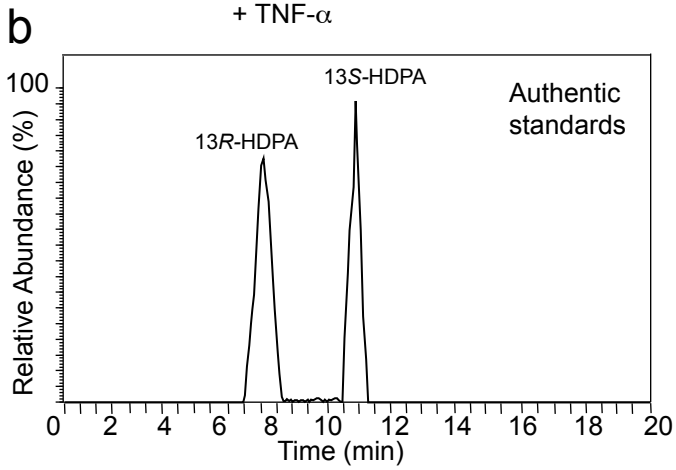
b
Relative Abundance (%)
100
13S-HDPA
13R-HDPA
Authentic
standards
0 2 4 6 8 10 12 14 16 18 20
Time (min)

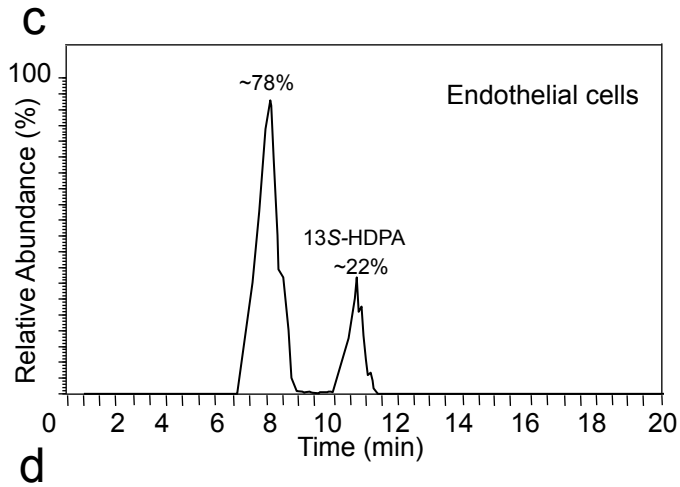
c
Relative Abundance (%)
100
~78%
Endothelial cells
13S-HDPA
~22%
0 2 4 6 8 10 12 14 16 18 20
Time (min)

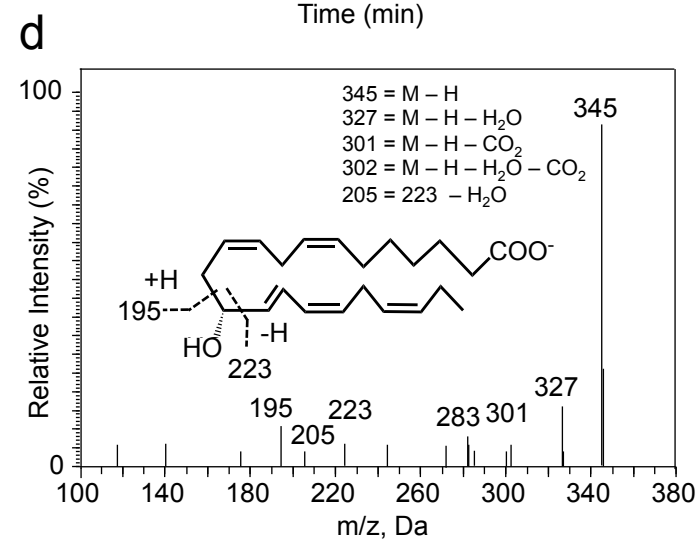
d
Relative Intensity (%)
100
345 = M – H
327 = M – H – H2O
301 = M – H – CO2
302 = M – H – H2O – CO2
205 = 223 – H2O
345
COO-
+H
195
HO
-H
223
327
195
223
205
283
301
0
100 140 180 220 260 300 340 380
m/z, Da

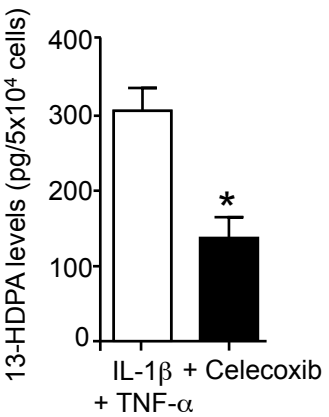
e
13-HDPA levels (pg/5x10^4 cells)
400
300
200
100
0
*
IL-1β + Celecoxib
+ TNF-α

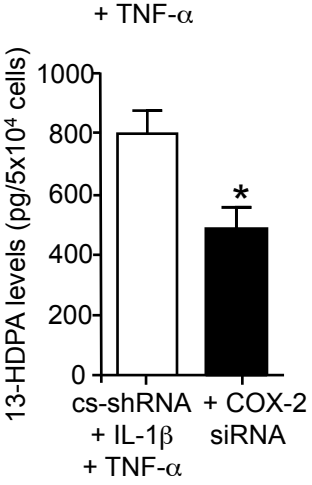
f
13-HDPA levels (pg/5x10^4 cells)
1000
800
600
400
200
0
*
cs-shRNA + COX-2
+ IL-1β siRNA
+ TNF-α

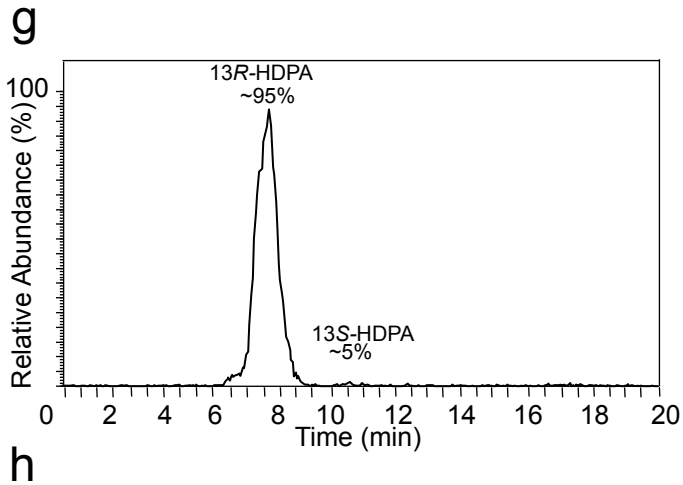
g
Relative Abundance (%)
100
13R-HDPA
~95%
13S-HDPA
~5%
0 2 4 6 8 10 12 14 16 18 20
Time (min)

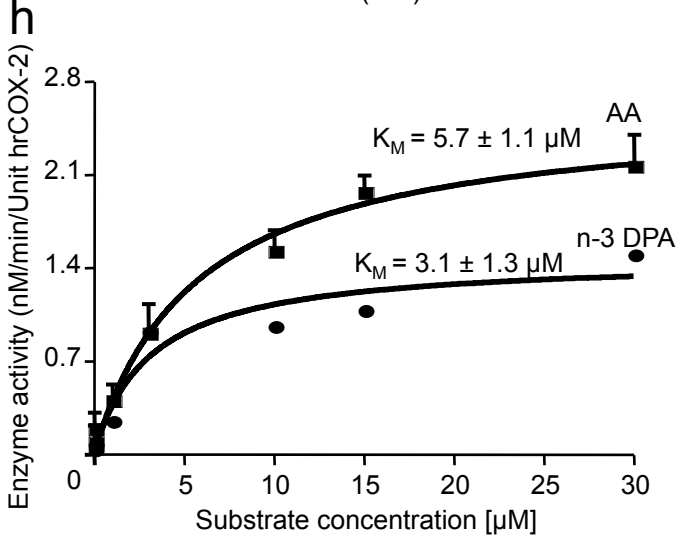
h
Enzyme activity (nM/min/Unit hrCOX-2)
2.8
2.1
1.4
0.7
0
AA
K_M = 5.7 ± 1.1 μM
n-3 DPA
K_M = 3.1 ± 1.3 μM
0 5 10 15 20 25 30
Substrate concentration [μM]

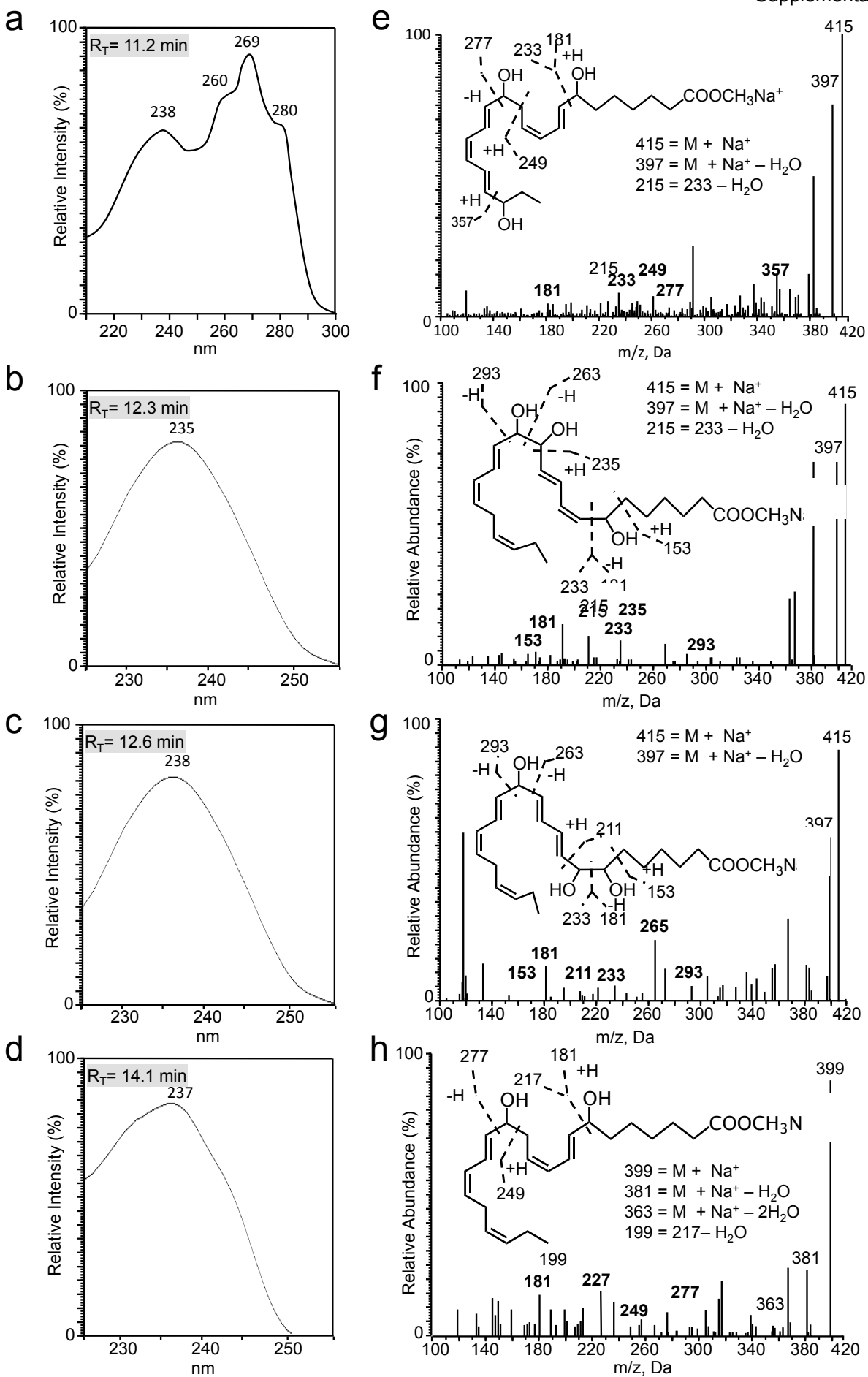
a
R_T= 11.2 min
238
260
269
280
Relative Intensity (%)
nm
b
R_T= 12.3 min
235
Relative Intensity (%)
nm
c
R_T= 12.6 min
238
Relative Intensity (%)
nm
d
R_T= 14.1 min
237
Relative Intensity (%)
nm
e
277
233
181
+H
OH
-H
OH
COOCH3Na+
+H
249
+H
357
OH
415 = M + Na+
397 = M + Na+ – H2O
215 = 233 – H2O
415
397
215
233
249
357
181
277
m/z, Da
f
293
-H
263
-H
OH
OH
+H
235
COOCH3N
OH
+H
153
-H
233
415 = M + Na+
397 = M + Na+ – H2O
215 = 233 – H2O
415
397
181
153
215
235
233
293
Relative Abundance (%)
m/z, Da
g
293
-H
OH
263
-H
+H
211
COOCH3N
HO
OH
153
-H
233
181
265
415 = M + Na+
397 = M + Na+ – H2O
415
181
153
211
233
293
Relative Abundance (%)
m/z, Da
h
277
181
+H
217
-H
OH
OH
COOCH3N
+H
249
199
399 = M + Na+
381 = M + Na+ – H2O
363 = M + Na+ – 2H2O
199 = 217– H2O
399
381
181
227
277
249
363
Relative Abundance (%)
m/z, Da

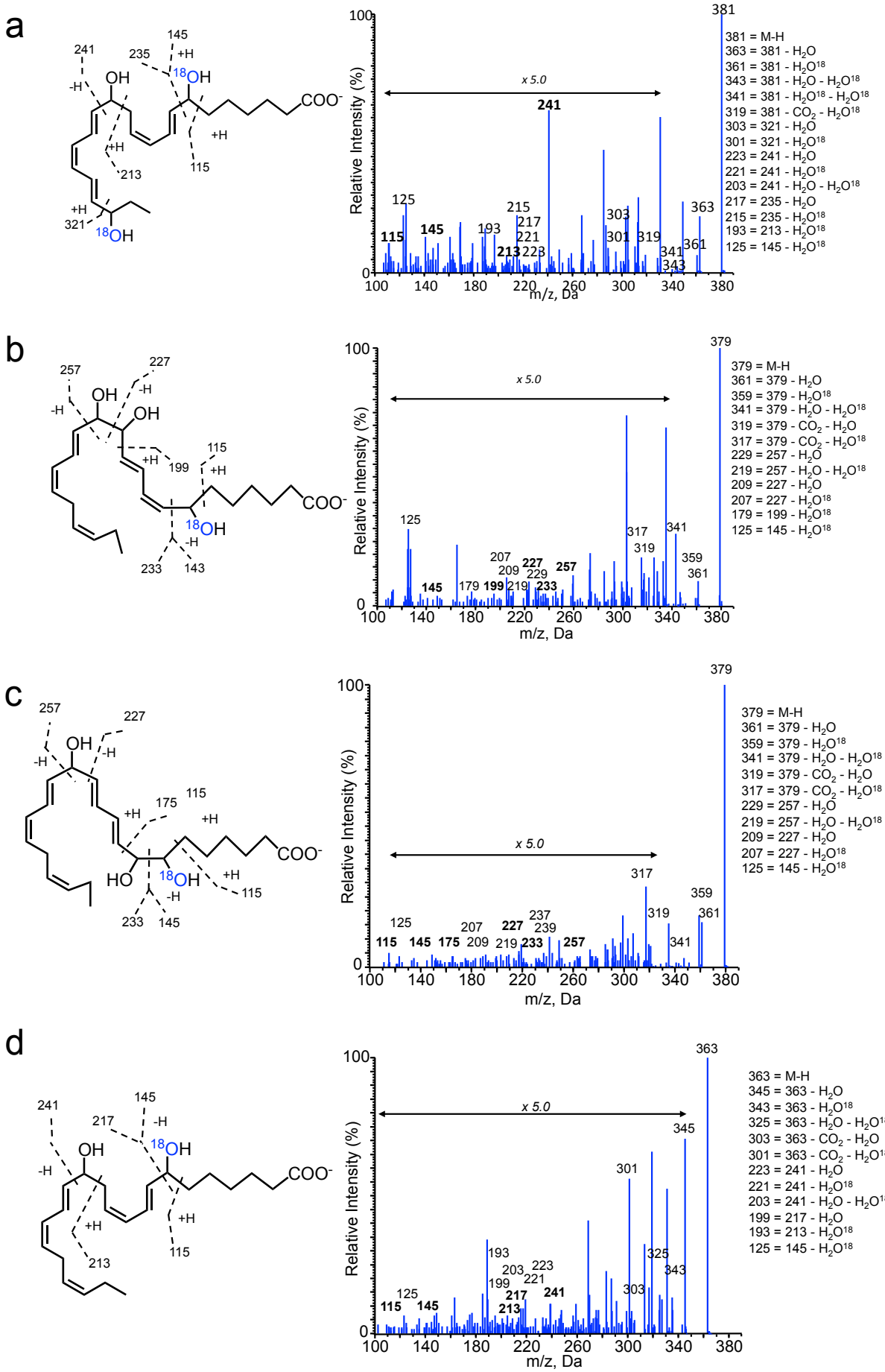
a
b
c
d
Relative Intensity (%)
m/z, Da
x 5.0
381 = M-H
363 = 381 - H2O
361 = 381 - H2O18
343 = 381 - H2O - H2O18
341 = 381 - H2O18 - H2O18
319 = 381 - CO2 - H2O18
303 = 321 - H2O
301 = 321 - H2O18
223 = 241 - H2O
221 = 241 - H2O18
203 = 241 - H2O - H2O18
217 = 235 - H2O
215 = 235 - H2O18
193 = 213 - H2O18
125 = 145 - H2O18
379 = M-H
361 = 379 - H2O
359 = 379 - H2O18
341 = 379 - H2O - H2O18
319 = 379 - CO2 - H2O
317 = 379 - CO2 - H2O18
229 = 257 - H2O
219 = 257 - H2O - H2O18
209 = 227 - H2O
207 = 227 - H2O18
179 = 199 - H2O18
125 = 145 - H2O18
379 = M-H
361 = 379 - H2O
359 = 379 - H2O18
341 = 379 - H2O - H2O18
319 = 379 - CO2 - H2O
317 = 379 - CO2 - H2O18
229 = 257 - H2O
219 = 257 - H2O - H2O18
209 = 227 - H2O
207 = 227 - H2O18
125 = 145 - H2O18
363 = M-H
345 = 363 - H2O
343 = 363 - H2O18
325 = 363 - H2O - H2O18
303 = 363 - CO2 - H2O
301 = 363 - CO2 - H2O18
223 = 241 - H2O
221 = 241 - H2O18
203 = 241 - H2O - H2O18
199 = 217 - H2O
193 = 213 - H2O18
125 = 145 - H2O18

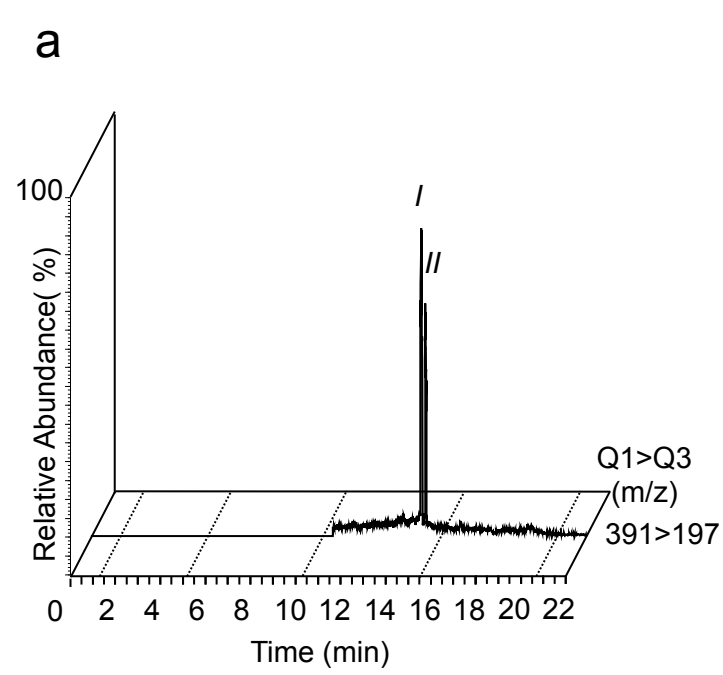
a
100
Relative Abundance(%)
I
II
Q1>Q3
(m/z)
391>197
0 2 4 6 8 10 12 14 16 18 20 22
Time (min)

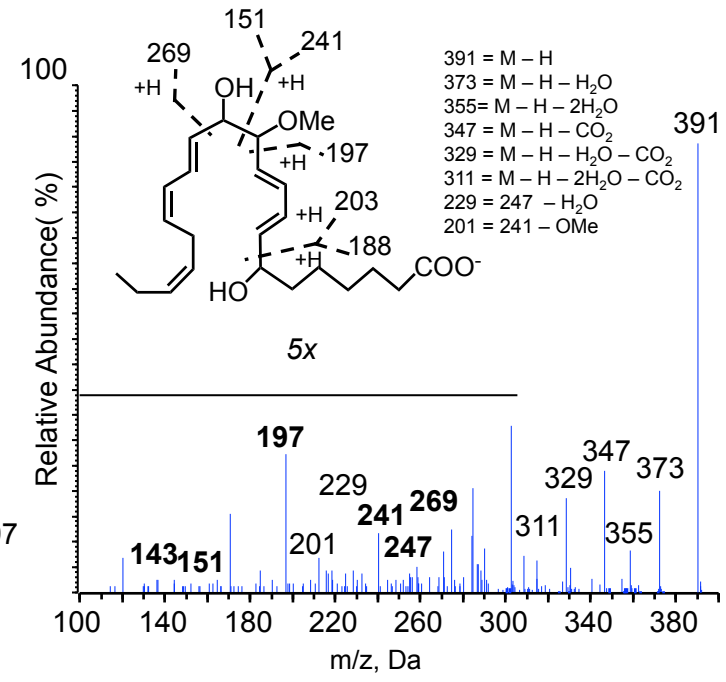
100
Relative Abundance(%)
151
241
269
+H
OH
+H
OMe
+H
197
+H
203
+H
188
+H
HO
COO-
391 = M – H
373 = M – H – H2O
355= M – H – 2H2O
347 = M – H – CO2
329 = M – H – H2O – CO2
311 = M – H – 2H2O – CO2
229 = 247 – H2O
201 = 241 – OMe
5x
197
229
241
269
201
247
143
151
311
347
329
373
355
100 140 180 220 260 300 340 380
m/z, Da

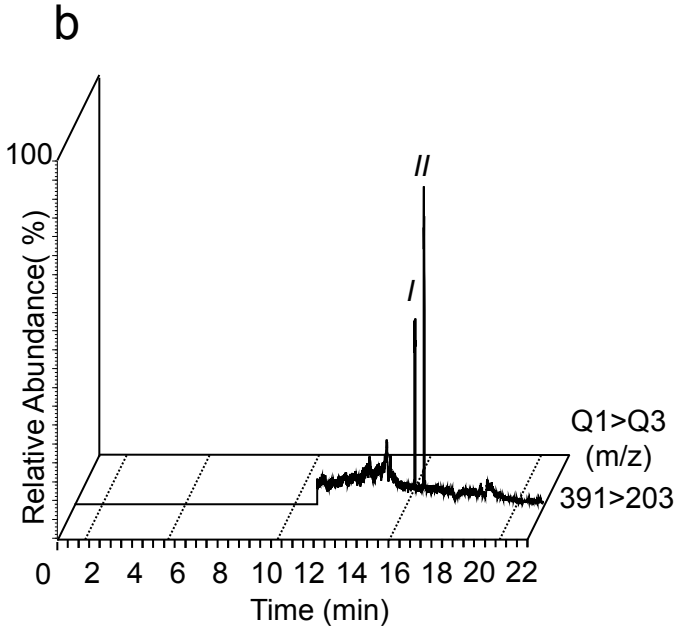
b
100
Relative Abundance(%)
II
I
Q1>Q3
(m/z)
391>203
0 2 4 6 8 10 12 14 16 18 20 22
Time (min)

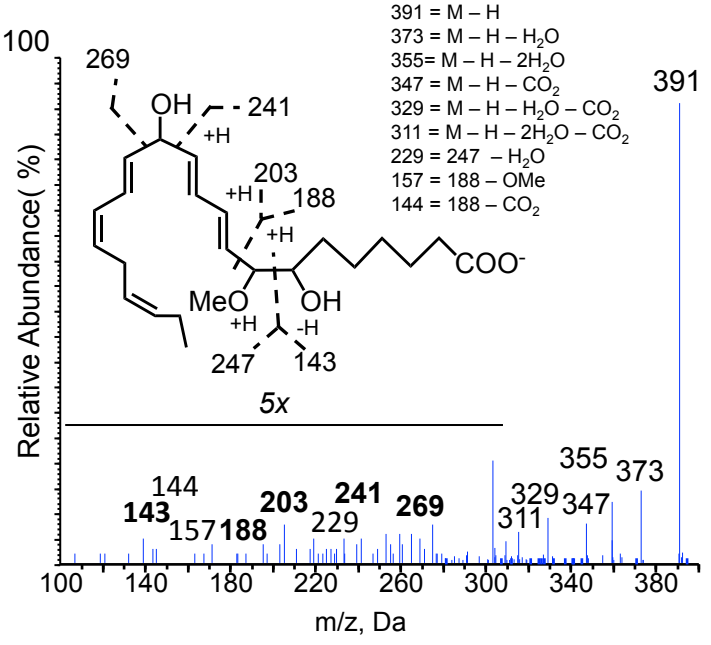
100
Relative Abundance(%)
269
OH
241
+H
203
+H
188
+H
COO-
MeO
+H
OH
-H
247
143
391 = M – H
373 = M – H – H2O
355= M – H – 2H2O
347 = M – H – CO2
329 = M – H – H2O – CO2
311 = M – H – 2H2O – CO2
229 = 247 – H2O
157 = 188 – OMe
144 = 188 – CO2
5x
144
143
157
188
203
229
241
269
311
329
347
355
373
100 140 180 220 260 300 340 380
m/z, Da

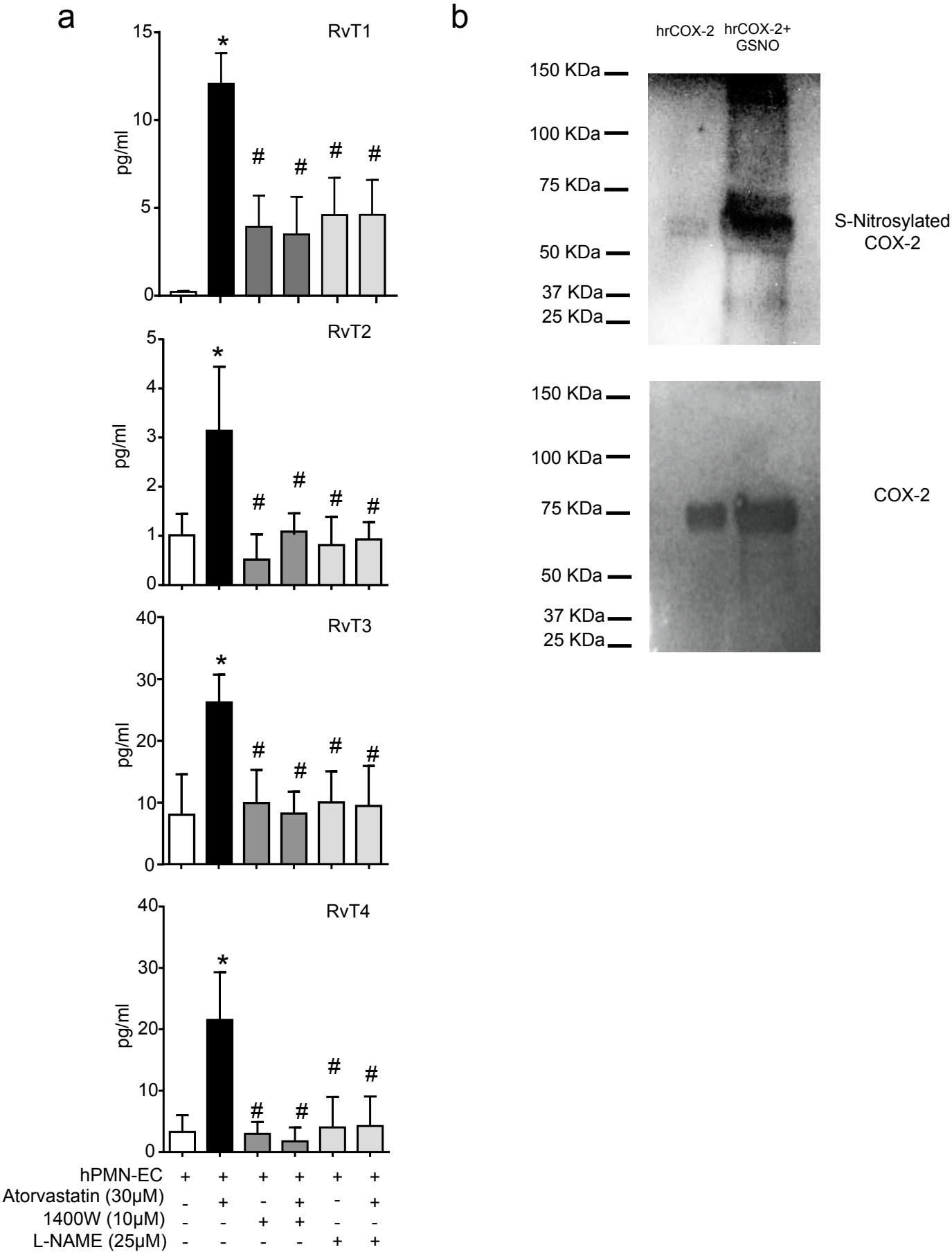
a
RvT1
RvT2
RvT3
RvT4
pg/ml
*
#
hPMN-EC + + + + + +
Atorvastatin (30μM) - + - + - +
1400W (10μM) - - + + - -
L-NAME (25μM) - - - - + +
b
hrCOX-2
hrCOX-2+ GSNO
150 KDa
100 KDa
75 KDa
50 KDa
37 KDa
25 KDa
S-Nitrosylated COX-2
COX-2

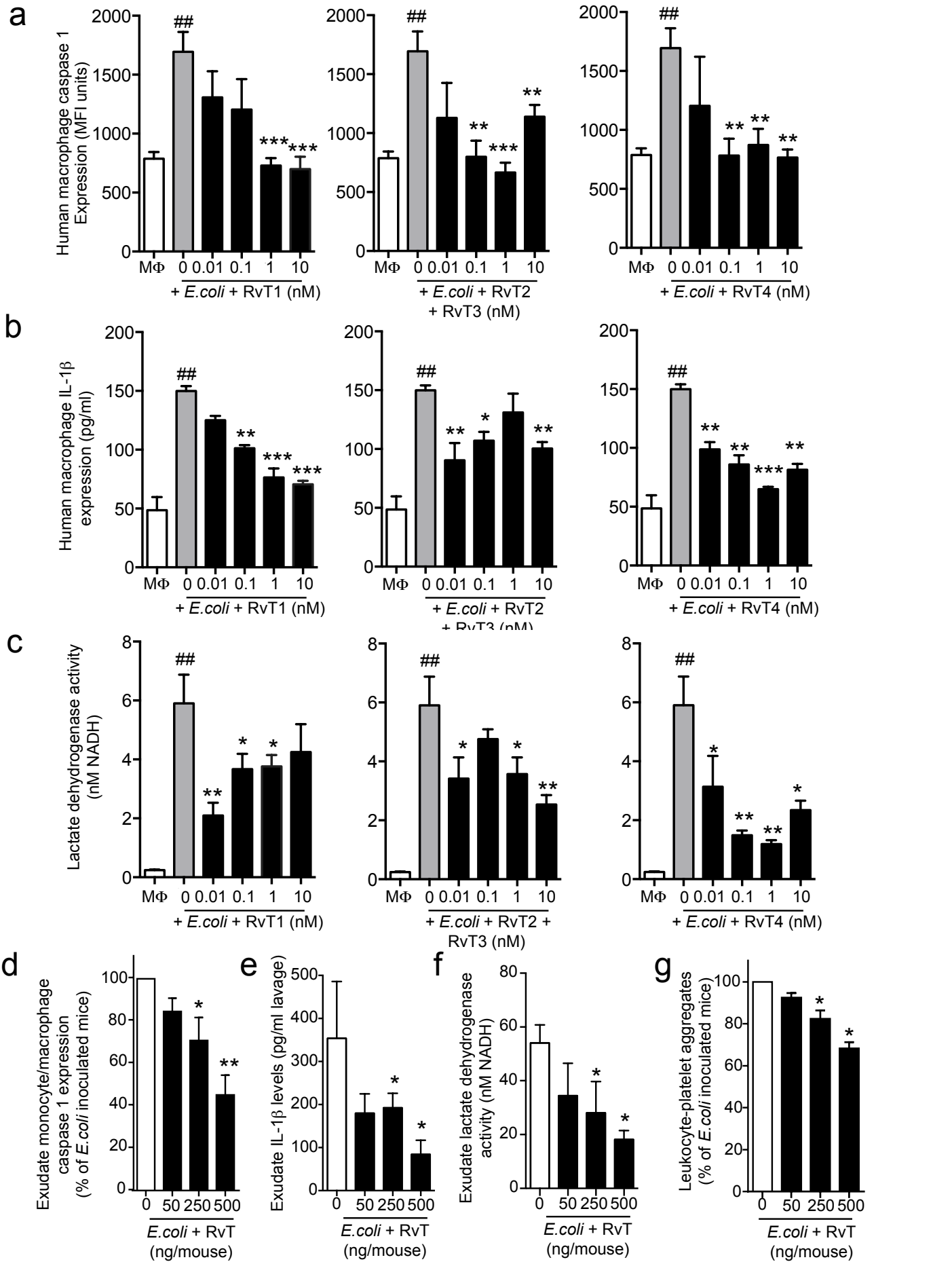
a
Human macrophage caspase 1 Expression (MFI units)
2000
1500
1000
500
0
##
***
**
MΦ 0 0.01 0.1 1 10
+ E.coli + RvT1 (nM)
+ E.coli + RvT2 + RvT3 (nM)
+ E.coli + RvT4 (nM)
b
Human macrophage IL-1β expression (pg/ml)
200
150
100
50
0
c
Lactate dehydrogenase activity (nM NADH)
8
6
4
2
0
d
Exudate monocyte/macrophage caspase 1 expression (% of E.coli inoculated mice)
100
80
60
40
20
0 50 250 500
E.coli + RvT (ng/mouse)
e
Exudate IL-1β levels (pg/ml lavage)
500
400
300
200
100
f
Exudate lactate dehydrogenase activity (nM NADH)
80
60
40
20
g
Leukocyte-platelet aggregates (% of E.coli inoculated mice)

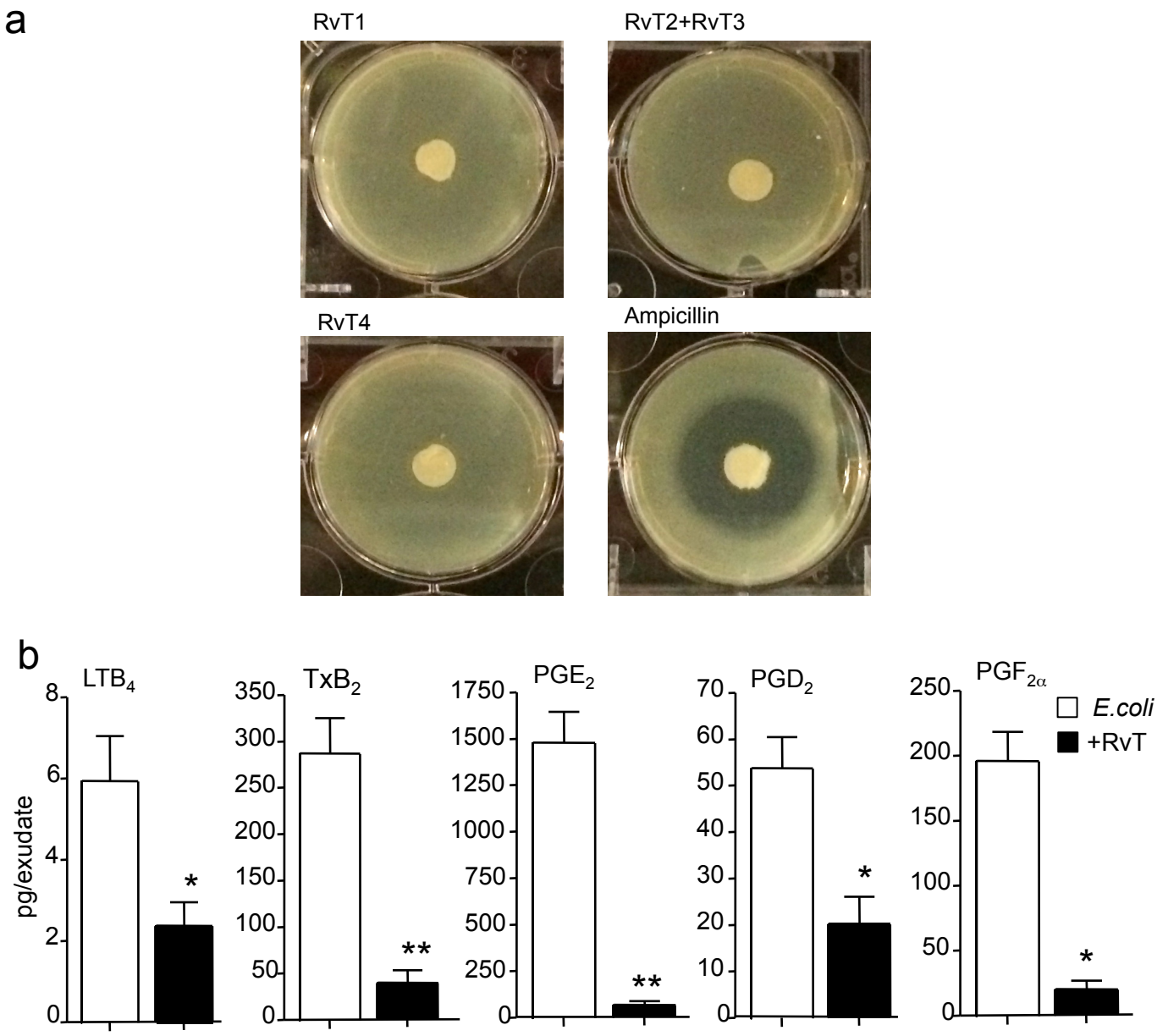
a
RvT1
RvT2+RvT3
RvT4
Ampicillin
b
LTB4
TxB2
PGE2
PGD2
PGF2α
pg/exudate
E.coli
+RvT
*
**

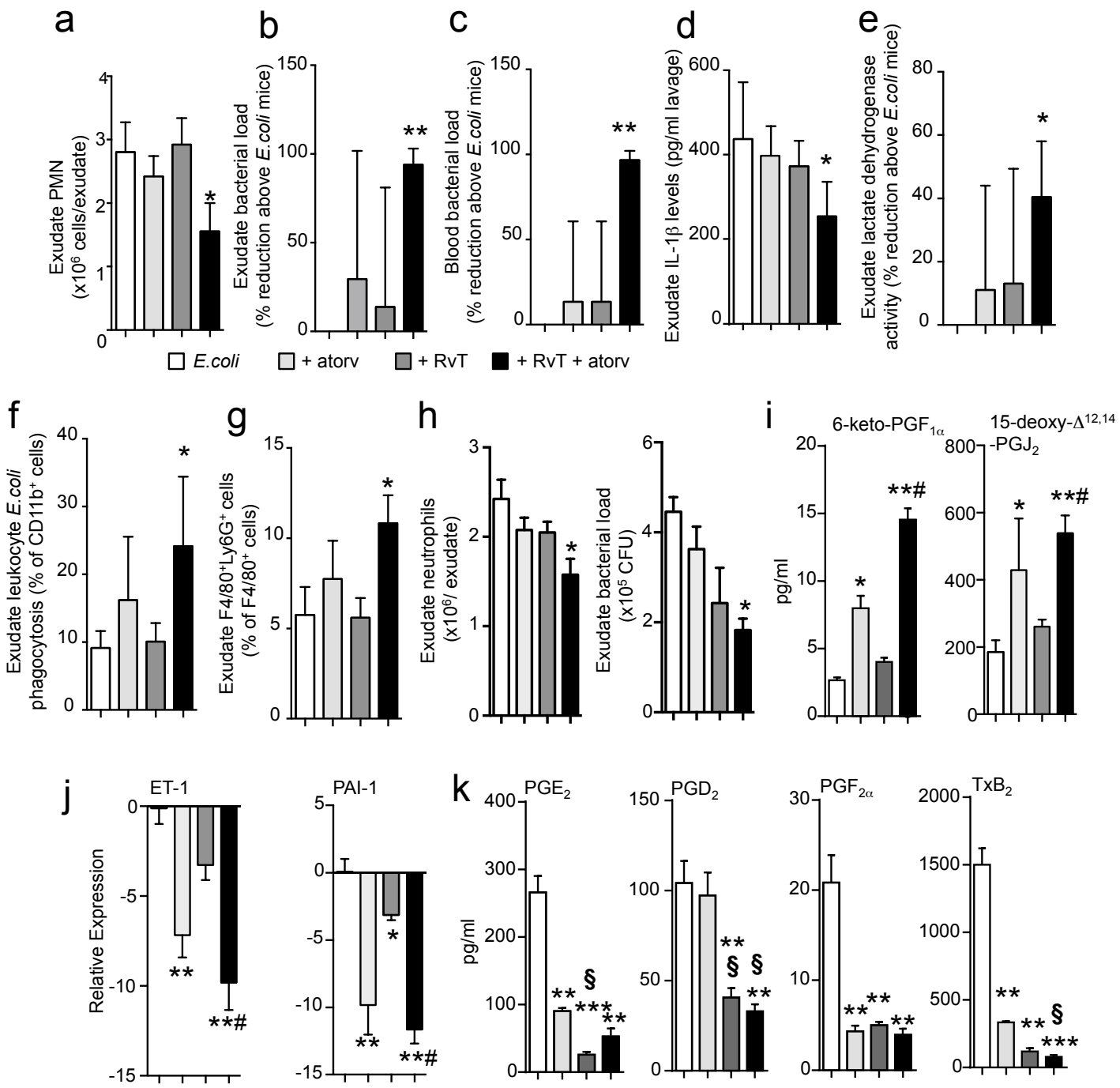
a
Exudate PMN (x10⁶ cells/exudate)
b
Exudate bacterial load (% reduction above E.coli mice)
c
Blood bacterial load (% reduction above E.coli mice)
d
Exudate IL-1β levels (pg/ml lavage)
e
Exudate lactate dehydrogenase activity (% reduction above E.coli mice)
E.coli
+ atorv
+ RvT
+ RvT + atorv
f
Exudate leukocyte E.coli phagocytosis (% of CD11b⁺ cells)
g
Exudate F4/80⁺Ly6G⁺ cells (% of F4/80⁺ cells)
h
Exudate neutrophils (x10⁶/ exudate)
Exudate bacterial load (x10⁵ CFU)
i
6-keto-PGF1α
15-deoxy-Δ12,14-PGJ2
pg/ml
j
ET-1
PAI-1
Relative Expression
k
PGE2
PGD2
PGF2α
TxB2
pg/ml

Supplementary Table 1: Peripheral blood lipid mediator profiles pre and post-exercise in healthy volunteers

a

Sex	Age (years)	Weight (Kg)	BMI (Kg/m^2)
2M/2F	30-46	64.8±5.4	22.7±0.7

b

DHA Bioactive Metabolome	**Pre-Exercise** (pg/ml)	**Post-Exercise** (pg/ml)
RvD1	1.0 ± 0.3	**4.6 ± 0.3**
RvD2	1.1 ± 0.3	**1.5 ± 0.4**
RvD3	0.4 ± 0.2	0.5 ± 0.2
RvD5	0.7 ± 0.2	0.9 ± 0.7
RvD6	37.8 ± 12.3	56.0 ± 23.3
MaR1	*	*
PD1	0.3 ± 0.1	0.5 ± 0.2
n-3 DPA Bioactive Metabolome		
RvT1	1.8 ± 0.8	**3.6 ± 0.4**
RvT2	0.6 ± 0.1	**2.7 ± 0.8**
RvT3	0.8 ± 0.4	**1.8 ± 0.5**
RvT4	0.8 ± 0.4	**1.8 ± 0.5**
EPA Bioactive Metabolome		
RvE1	0.6 ± 0.2	1.5 ± 0.9
RvE2	39.1 ± 19.3	32.5 ± 23.4
RvE3	29.1 ± 11.1	69.3 ± 14.6
AA Bioactive Metabolome		
LXA_4	3.6 ± 1.7	8.0 ± 5.3
LXB_4	7.4 ± 4.0	19.3 ± 8.4
5,15-diHETE	74.0 ± 22.6	89.1 ± 52.7
LTB_4	4.5 ± 1.7	14.4 ± 7.0
PGD_2	6.5 ± 2.7	31.2 ± 16.8
PGE_2	115.2 ± 59.8	148.4 ± 78.5
PGF_{2a}	4.4 ± 1.5	12.9 ± 10.3
8-iso-PGF_{2a}	6.6 ± 5.4	3.9 ± 2.3
TxB_2	4.8 ± 4.1	**36.2 ± 9.9**
12-HHT	109.0 ± 68.1	177.6 ± 55.1

(**a**) Healthy volunteer demographics (**b**) Peripheral blood was collected from healthy volunteers pre- and post-exercise (see methods) and lipid mediator levels quantified using MRM monitoring of the parent ion in Q1 and a characteristic fragment ion in Q3. Results are expressed as mean ± s.e.m. n=4 healthy volunteers from four independent experiments. * = below limits; limits ~0.1pg. Numbers denoted in bold are $p< 0.05$ *vs.* pre-exercise values

Supplementary Table 2: Comparison of SPM and Eicosanoids versus novel RvT in plasma from healthy volunteers and sepsis patients

a

Samples	Sex	Age (years)	Blood Culture
Sepsis Patients	5F/5M	57-96	1/10 *Salmonella* sp 1/10 *Streptococcus pyogenes* 2/10 *Staphylococcus hominis* 3/10 *Corynebacterium* sp. 1/10 *S. infantarius* 1/10 *S. viridans* 1/10 *S maltophilla*
Healthy	3F/3M	33-65	N/A
SRM 1950	50M/50F	40-50	N/A

b

DHA Bioactive Metabolome	**Reference Plasma** (pg/ml)	**Healthy Volunteer Plasma** (pg/ml)	**Sepsis Patients Plasma** (pg/ml)
RvD1	0.8 ± 0.4	1.8 ± 1.4	**4.6 ± 2.4**
RvD2	0.9 ± 0.3	1.5 ± 1.0	**3.7 ± 1.3**
RvD3	*	*	**10.5 ± 5.5**
RvD5	0.8 ± 0.3	0.9 ± 0.5	**17.0 ± 6.9**
RvD6	1.5 ± 0.2	**27.6 ± 7.2**	**121.8 ± 31.8**
MaR1	*	*	**7.4 ± 3.4**
PD1	*	1.2 ± 0.8	1.5 ± 0.7
n-3 DPA Bioactive Metabolome			
RvT1	5.0 ± 1.7	**2.9 ± 0.6**	**6.6 ± 1.1**
RvT2	2.2 ± 1.3	1.2 ± 0.3	**10.0 ± 1.8**
RvT3	1.0 ± 0.2	0.9 ± 0.4	**17.5 ± 3.2**
RvT4	7.3 ± 3.1	**1.4 ± 0.6**	**15.2 ± 3.3**
EPA Bioactive Metabolome			
RvE1	*	2.2 ± 1.2	**11.0 ± 5.3**
RvE2	*	**3.7 ± 0.9**	**24.7 ± 11.2**
RvE3	1.5 ± 0.5	**8.9 ± 2.6**	**361.3 ± 241.5**
AA Bioactive Metabolome			
LXA_4	*	0.8 ± 0.4	**5.5 ± 2.4**
LXB_4	8.7 ± 2.7	3.2 ± 1.5	**56.7 ± 20.5**
5,15-diHETE	4.2 ± 1.7	6.2 ± 1.1	87.1 ± 55.7
LTB_4	25.2 ± 3.1	3.7 ± 2.2	3.3 ± 1.2
PGD_2	7.3 ± 1.2	9.8 ± 4.4	**79.4 ± 24.1**
PGE_2	17.8 ± 5.1	24.1 ± 9.7	**132.1 ± 22.2**
PGF_{2a}	1.7 ± 0.7	4.2 ± 0.6	**51.0 ± 10.2**
8-iso-$PGF_{2\alpha}$	4.5 ± 1.0	1.9 ± 1.0	11.8 ± 5.3
TxB_2	6.3 ± 3.2	10.5 ± 6.3	**185.4 ± 96.5**
12-HHT	21.8 ± 1.0	39.6 ± 13.8	**127.7 ± 89.9**

(**a**) healthy volunteer demographics and patient demographics and cultures. (**b**) Plasma was obtained from the NIST repository (reference plasma; d=3), collected from healthy volunteers (n=4) or patients diagnosed with sepsis (n=9), and lipid mediator levels quantified using MRM monitoring of the parent ion in Q1 and a characteristic fragment ion in Q3. Results are expressed as mean±s.e.m. from two independent experiments. * = below limits; limits ~0.1pg. Numbers denoted in bold are $p < 0.05$ *vs* reference plasma values.

Supplementary Table 2: Peripheral blood lipid mediator profiles during self-resolving infections in mice

DHA Bioactive Metabolome	**0h** (pg/ml)	**4h** (pg/ml)	**12h** (pg/ml)	**24h** (pg/ml)	**48h** (pg/ml)
RvD1	5.5 ± 3.5	51.0 ± 22.8	**27.6 ± 13.6**	**12.8 ± 2.8**	15.5 ± 7.4
RvD2	8.1 ± 3.2	16.0 ± 6.1	**22.7 ± 5.2**	**4.0 ± 0.9**	**2.2 ± 0.9**
RvD3	2.6 ± 1.0	6.3 ± 3.4	**2.7 ± 0.6**	**1.1 ± 0.3**	**6.1 ± 4.6**
RvD5	22.7 ± 4.4	16.9 ± 2.5	**25.1 ± 8.1**	**8.7 ± 1.0**	**9.2 ± 1.7**
RvD6	51.4 ± 18.4	**346.8 ± 82.5**	**435.8 ± 51.6**	**259.3 ± 49.3**	**219.4 ± 60.7**
MaR1	*	*	*	*	*
PD1	1.8 ± 1.2	4.2 ± 1.8	4.1 ± 1.4	3.0 ± 0.8	3.9 ± 1.2
n-3 DPA Bioactive Metabolome					
RvT1	6.4 ± 2.1	**34.6 ± 3.3**	12.6 ± 2.9	6.8 ± 2.6	10.3 ± 3.3
RvT2	9.4 ± 3.2	**50.3 ± 10.0**	14.1 ± 2.3	5.2 ± 1.2	**5.2 ± 0.8**
RvT3	11.5 ± 6.0	**32.7 ± 4.6**	16.4 ± 1.3	3.3 ± 1.1	**5.2 ± 1.1**
RvT4	10.2 ± 1.5	**45.5 ± 3.5**	10.4 ± 1.7	5.1 ± 1.4	**4.8 ± 0.5**
EPA Bioactive Metabolome					
RvE1	0.6 ± 0.4	0.2 ± 0.3	2.2 ± 2.6	0.6 ± 0.2	2.7 ± 1.2
RvE2	14.0 ± 2.2	88.5 ± 26.3	**139.0 ± 37.1**	85.0 ± 27.9	44.4 ± 17.9
RvE3	39.4 ± 4.5	**229.4 ± 47.9**	**356.3 ± 51.7**	**155.7 ± 20.2**	104.9 ± 40.5
AA Bioactive Metabolome					
LXA_4	12.6 ± 4.1	39.9 ± 23.7	**70.7 ± 26.8**	16.7 ± 5.3	46.0 ± 15.1
LXB_4	41.1 ± 13.5	73.9 ± 22.4	**143.9 ± 59.7**	37.2 ± 8.5	36.2 ± 7.0
5,15-diHETE	95.0 ± 4.6	121.1 ± 19.7	**51.6 ± 20.5**	36.4 ± 9.1	**19.2 ± 4.3**
LTB_4	0.7 ± 0.4	**100.3 ± 18.2**	**35.9 ± 6.7**	12.0 ± 2.8	106.9 ± 42.0
PGD_2	7.7 ± 0.9	**353.5 ± 11.5**	**273.4 ± 50.0**	77.3 ± 20.6	**106.3 ± 17.7**
PGE_2	9.2 ± 1.4	**1602.0 ± 517.9**	**1775.6 ± 302.8**	323.0 ± 196.8	**414.3 ± 117.2**
$PGF_{2\alpha}$	3.3 ± 0.1	**153.0 ± 64.5**	**57.5 ± 19.4**	12.2 ± 3.3	**26.7 ± 6.5**
8-iso-$PGF_{2\alpha}$	8.1 ± 0.9	**227.6 ± 45.6**	**255.0 ± 96.6**	64.5 ± 16.8	71.6 ± 25.3
TxB_2	24.9 ± 9.5	**1773.7 ± 514.9**	**471.4 ± 174.6**	**214.3 ± 26.0**	**176.5 ± 22.0**
12-HHT	89.8 ± 24.2	**12598.1 ± 4257.8**	**12879.5 ± 772.7**	**3208.8 ± 871.5**	**4237.5 ± 750.0**

Mice were inoculated with *E.coli* ($1x10^5$ CFU/mouse), blood was collected at the indicated intervals and lipid mediator levels quantified using MRM monitoring of the parent ion in Q1 and a characteristic fragment ion in Q3. Results are expressed as mean ± s.e.m. n=4 mice per group from two independent experiments. * = below limits; limits ~0.1pg. Numbers denoted in bold are $p< 0.05$ *vs.* 0h values.

Supplementary Table 3: Mouse peripheral blood lipid mediator profiles during self-resolving and delayed-resolving infections

DHA Bioactive Metabolome	Self-Resolving Infections	Delayed-Resolving Infections
RvD1	9.8 ± 1.1	**3.5 ± 1.3**
RvD2	9.4 ± 2.6	7.4 ± 1.5
RvD3	5.7 ± 1.2	**1.3 ± 0.2**
RvD5	63.6 ± 13.8	113.2 ± 29.1
RvD6	55.2 ± 3.7	**20.6 ± 10.4**
MaR1	0.3 ± 0.1	0.2 ± 0.2
PD1	4.2 ± 1.1	6.9 ± 3.0
n-3 DPA Bioactive Metabolome		
RvT1	40.6 ± 9.4	**19.9 ± 3.6**
RvT2	55.8 ± 9.1	**21.7 ± 2.9**
RvT3	41.8 ± 3.5	**7.9 ± 1.8**
RvT4	36.4 ± 2.0	**19.7 ± 3.9**
EPA Bioactive Metabolome		
RvE1	21.5 ± 6.8	**13.0 ± 2.6**
RvE2	5.2 ± 1.6	**2.8 ± 0.9**
RvE3	39.0 ± 14.0	32.6 ± 8.7
AA Bioactive Metabolome		
LXA_4	3.2 ± 1.1	2.6 ± 1.6
LXB_4	50.7 ± 5.7	**25.1 ± 5.1**
5,15-diHETE	22.6 ± 6.4	29.2 ± 13.2
LTB_4	0.5 ± 0.0	2.3 ± 0.6
PGD_2	6.3 ± 2.3	**14.3 ± 1.7**
PGE_2	2.7 ± 0.8	**6.7 ± 2.8**
PGF_{2a}	2.1 ± 0.6	1.5 ± 0.4
8-iso-$PGF_{2\alpha}$	4.4 ± 2.2	**20.1 ± 1.5**
TxB_2	4.4 ± 2.2	**21.6 ± 2.6**
12-HHT	12.3 ± 2.0	**31.3 ± 3.8**

Mice were inoculated with $1x10^5$ CFU/mouse *E.coli* (self-resolving) or $1x10^7$ CFU/mouse *E.coli* (delayed-resolving), blood was collected after 4h and lipid mediator levels quantified using MRM monitoring of the parent ion in Q1 and a characteristic fragment ion in Q3. Results are expressed as mean±s.e.m. n=5 mice per group from two independent experiments. Numbers denoted in bold are $p< 0.05$ *vs.* self-resolving values.

Supplementary Table 4: Lipid mediator levels in human endothelial cell incubations and neutrophil-endothelial cell co-incubations.

DHA Bioactive Metabolome	Endothelial cells	Neutrophil-endothelial cells	Neutrophil-endothelial cells plus Atorvastatin
RvD1	2.5 ± 1.7	1.8 ± 1.8	0.3 ± 0.1
RvD2	6.4 ± 0.9	4.3 ± 0.9	6.4 ± 1.9
RvD3	11.8 ± 2.8	7.5 ± 1.2	8.9 ± 3.2
RvD5	11.3 ± 1.4	10.7 ± 1.7	**8.2 ± 1.4**
RvD6	84.5 ± 14.7	108.2 ± 29.7	**122.8 ± 16.0**
MaR1	7.1 ± 2.2	4.8 ± 1.6	6.8 ± 2.0
PD1	0.7 ± 0.5	0.2 ± 0.1	0.2 ± 0.0
n-3 DPA Bioactive Metabolome			
RvT1	1.7 ± 0.5	**8.4 ± 1.0**	**13.4 ± 0.9**
RvT2	1.3 ± 0.8	**3.2 ± 1.6**	**17.7 ± 3.0**
RvT3	2.5 ± 0.8	**8.8 ± 1.8**	**15.9 ± 4.2**
RvT4	3.0 ± 0.3	**11.3 ± 1.7**	**13.7 ± 1.3**
EPA Bioactive Metabolome			
RvE1	0.0 ± 0.0	0.5 ± 0.4	2.0 ± 1.5
RvE2	42.0 ± 24.2	32.7 ± 8.6	**71.7 ± 20.8**
RvE3	18.1 ± 1.8	27.5 ± 9.1	**25.4 ± 6.3**
AA Bioactive Metabolome			
LXA_4	33.1 ± 6.1	26.8 ± 5.8	21.0 ± 2.8
LXB_4	4.5 ± 2.6	13.5 ± 9.1	10.1 ± 7.0
5,15-diHETE	17.8 ± 3.5	20.8 ± 4.1	21.2 ± 1.5
LTB_4	0.4 ± 0.2	**50.8 ± 9.9**	**63.8 ± 11.3**
PGD_2	35.1 ± 8.2	**132.1 ± 30.5**	**120.0 ± 40.4**
PGE_2	46.7 ± 6.8	**481.0 ± 114.6**	**414.4 ± 193.5**
PGF_{2a}	790.7 ± 152.0	**1115.4 ± 76.6**	**1064.2 ± 168.8**
8-iso-$PGF_{2\alpha}$	13.3 ± 4.0	22.0 ± 1.3	21.9 ± 10.8
TxB_2	367.5 ± 82.7	**1680.8 ± 252.2**	**1367.0 ± 420.1**
12-HHT	102.0 ± 21	**819.0 ± 318.9**	**1005.3 ± 459.2**

Human endothelial cells were incubated with IL1β and TNF-α (10ng/ml each, 16h, 37°C), then vehicle (PBS containing 0.01% EtOH) or atorvastatin (Atorv; 30 min), for 30 min followed by n-3 DPA (1μM, 15min, 37°C) and human neutrophils ($1x10^7$ cells/ml, 60min, 37°C) or PBS. Products were profiled using LM metabololipidomics and quantified using MRM monitoring of the parent ion in Q1 and a characteristic fragment ion in Q3. Results are mean ± s.e.m. n=4 independent cell preparations per group from four independent experiments. Numbers denoted in bold are $p< 0.05$ *vs.* endothelial cell incubations alone.

Table S5: Evidence for the structure, biosynthesis, and actions of 13-series resolvins.

	Biological system identified	For structural elucidation	Biosynthesis	Bioactions	
				In vivo	In vitro
RvT1	• Human healthy volunteer whole blood • Human sepsis patient plasma • Mouse plasma during *E.coli* infections • Human neutrophil and endothelial cell co-incubations	• Retention time in liquid chromatography 11.2 min • UV chromophore λ_{max}[#] 269 and 238nm • MS-MS spectrum of natural product m/z 377, 359, 341, 333, 319, 297, 239, 233, 215, 211, 193, 175, 143 • MS-MS spectrum of methyl ester sodium adduct m/z 415, 397, 357, 277, 249, 233, 181 • MS-MS spectrum of product containing O^{18}: m/z 381, 363, 361, 343, 341, 319, 303, 301, 241, 223, 221, 217, 215, 213, 193, 145, 125, 115	• Addition of n-3 docosapentaenoic acid to neutrophil-endothelial co-incubations increased compound 1 levels • COX-2 specific inhibitor and shRNA to human COX-2 reduced 13R-hydroxy-7Z,10Z,14,16Z,19Z- docosapentaenoic acid levels • COX-2 specific inhibitor reduced compound 1 levels in human neutrophil-endothelial cell co-incubations • O^{18} incorporation	• Protects against infection induced hypothermia* • Limits neutrophil recruitment during infections* • Stimulates murine leukocyte phagocytosis of *E.coli** • Stimulates macrophage efferocytosis of apoptotic neutrophils* • Reduces exudate pro-inflammatory eicosanoid levels during infections* • Reduces levels of inflammasome components* • Reduces pyroptosis • Elaborates the protective actions of atorvastatin in infections* • Reduces circulating platelet-leukocyte aggregates* • Downregulation of ET-1 and PAI-1 in lung tissue*	• Stimulates human macrophage efferocytosis of apoptotic neutrophils • Stimulates human macrophage and neutrophil phagocytosis of *E.coli* • Stimulates human macrophage and neutrophil intra-phagolysosomal ROS production • Reduces *E.coli* induced inflammasome components in human macrophages • Reduces *E.coli* induced macrophage pyroptosis
RvT2	• Human healthy volunteer whole blood • Human sepsis patient plasma • Mouse plasma during *E.coli* infections • Human neutrophil and endothelial cell co-incubations	• Retention time in liquid chromatography 12.3 min • UV chromophore λ_{max}[#] 235 nm • MS-MS spectrum m/z 377, 359, 341, 333, 315, 297, 233, 225, 207, 197, 181, 143 • MS-MS spectrum of methyl ester sodium adduct m/z 415, 397, 293, 235, 233, 181,153 • MS-MS spectrum of product containing O^{18}: m/z 379, 361, 359, 319, 317, 257, 233, 229, 227, 219, 209, 207, 199, 179, 145, 125	• Addition of n-3 docosapentaenoic acid to neutrophil-endothelial co-incubations increased compound 1 levels • COX-2 specific inhibitor and shRNA to human COX-2 reduced 13R-hydroxy-7Z,10Z,14,16Z,19Z-docosapentaenoic acid levels • COX-2 specific inhibitor reduced compound 1 levels in human neutrophil-endothelial cell co-incubations • Incubation of 13R-hydroxy-7Z,10Z,14,16Z,19Z-docosapentaenoic acid with neutrophils and acid methanol gave trapping products that were consistent with the formation of an epoxide intermediate • O^{18} incorporation	• Protects against infection induced hypothermia* • Limits neutrophil recruitment during infections* • Stimulates murine leukocyte phagocytosis of *E.coli** • Stimulates macrophage efferocytosis of apoptotic neutrophils* • Reduces exudate pro-inflammatory eicosanoid levels during infections* • Reduces levels of inflammasome components* • Reduces pyroptosis • Elaborates the protective actions of atorvastatin in infections* • Downregulation of ET-1 and PAI-1 in lung tissue • Reduces circulating platelet - leukocyte aggregates*	• Stimulates human macrophage efferocytosis of apoptotic neutrophils • Stimulates human macrophage and neutrophil phagocytosis of *E.coli* • Stimulates human macrophage and neutrophil intra-phagolysosomal ROS production • Reduces *E.coli* induced inflammasome components in human macrophages • Reduces *E.coli* induced macrophage pyroptosis

RvT3	• Human healthy volunteer whole blood • Human sepsis patient plasma • Mouse plasma during *E.coli* infections • Human neutrophil and endothelial cell co-incubations	• Retention time in liquid chromatography 12.6 min • UV chromophore λ_{max}# 238 nm • MS-MS spectrum 377, 359, 341, 333, 315, 297, 255, 233, 207, 173, 155, 143 • MS-MS spectrum of methyl ester sodium adduct m/z 415, 397, 293, 265, 233, 211, 181 • MS-MS Spectrum of product containing O^{18}: m/z 379, 361, 359, 341, 319, 317, 257, 239, 237, 233, 227, 219, 209, 207, 175, 145, 125, 115	• Addition of n-3 docosapentaenoic acid to neutrophil-endothelial co-incubations increased compound 1 levels • COX-2 specific inhibitor and shRNA to human COX-2 reduced 13R-hydroxy-7Z,10Z,14,16Z,19Z- docosapentaenoic acid levels • COX-2 specific inhibitor reduced compound 1 levels in human neutrophil-endothelial cell co-incubations • Incubation of 13R-hydroxy-7Z,10Z,14,16Z,19Z- docosapentaenoic acid with neutrophils and acid methanol gave trapping products that were consistent with the formation of an epoxide intermediate • O^{18} incorporation	• Protects against infection induced hypothermia* • Limits neutrophil recruitment during infections* • Stimulates murine leukocyte phagocytosis of *E.coli** • Stimulates macrophage efferocytosis of apoptotic neutrophils* • Reduces exudate pro-inflammatory eicosanoid levels during infections* • Reduces levels of inflammasome components* • Reduces pyroptosis • Elaborates the protective actions of atorvastatin in infections* • Reduces circulating platelet-leukocyte aggregates* • Downregulation of ET-1 and PAI-1 in lung tissue*	• Stimulates human macrophage efferocytosis of apoptotic neutrophils • Stimulates human macrophage and neutrophil phagocytosis of *E.coli* • Stimulates human macrophage and neutrophil intra-phagolysosomal ROS production • Reduces *E.coli* induced inflammasome components in human macrophages • Reduces *E.coli* induced macrophage pyroptosis
RvT4	• Human healthy volunteer whole blood • Human sepsis patient plasma • Mouse plasma during *E.coli* infections • Human neutrophil and endothelial cell co-incubations	• Retention time in liquid chromatography 14.1 min • UV chromophore λ_{max}# 237 nm • MS-MS spectrum m/z 361, 343, 325, 299, 221, 239, 217, 211, 199, 193, 143 • MS-MS spectrum of methyl ester sodium adduct m/z 399, 381, 363, 249, 227, 199, 181 • MS-MS spectrum of product containing O^{18}: m/z 363, 345, 343, 325, 303, 301 241, 233, 221, 217, 213, 203, 199, 193, 145, 125, 115	• Addition of n-3 docosapentaenoic acid to neutrophil-endothelial co-incubations increased compound 1 levels • COX-2 specific inhibitor and shRNA to human COX-2 reduced 13R-hydroxy-7Z,10Z,14,16Z,19Z- docosapentaenoic acid levels • COX-2 specific inhibitor reduced compound 1 levels in human neutrophil-endothelial cell co-incubations • O^{18} incorporation	• Protects against infection induced hypothermia* • Limits neutrophil recruitment during infections* • Stimulates murine leukocyte phagocytosis of *E.coli** • Stimulates macrophage efferocytosis of apoptotic neutrophils* • Reduces exudate pro-inflammatory eicosanoid levels during infections* • Reduces levels of inflammasome components* • Reduces pyroptosis • Elaborates the protective actions of atorvastatin in infections* • Reduces circulating platelet-leukocyte aggregates* • Downregulation of ET-1 and PAI-1 in lung tissue*	• Stimulates human macrophage efferocytosis of apoptotic neutrophils • Stimulates human macrophage and neutrophil phagocytosis of *E.coli* • Stimulates human macrophage and neutrophil intra-phagolysosomal ROS production • Reduces *E.coli* induced inflammasome components in human macrophages • Reduces *E.coli* induced macrophage pyroptosis

n = 3 or greater for experiments for structure elucidation. n = 3–4 for human neutrophil and macrophage assays and n= 4-17 for in vivo experiments. *These bioactions were determined following co-administration of RvT1, RvT2, RvT3 and RvT4.

#Spectra were recorded online in methanol/water using an Agilent Technologies 1100 series diode array detector.